THEORETICAL & APPLIED MECHANICS LETTERS **4**, 062004 (2014)

On properties of the deterministic turbulence and reproducibility of its instantaneous and statistical characteristics

Vladimir I. Borodulin,[a] Yury S. Kachanov[b]
Khristianovich Institute of Theoretical and Applied Mechanics of the Russian Academy of Sciences, Novosibirsk 630090, Russia

(Received 8 October 2014; revised 6 November 2014; accepted 7 November 2014)

Abstract As known from previous studies, the deterministic turbulence (DeTu) is a post-transitional flow that is turbulent according to the generally accepted statistical characteristics but possesses, meanwhile, a significant degree of determinism, i.e., reproducibility of its instantaneous structure. It is found that the DeTu can occur in those cases when transition is caused by convective instabilities; in boundary layers, in particular. The present paper is devoted to a brief description of history of discovering the DeTu phenomenon, as well as to some recent advance in investigation of instantaneous and statistical properties of such turbulent boundary layer flows.
 [doi:10.1063/2.1406204]

Keywords boundary layer, laminar-turbulent transition, deterministic wall turbulence, instantaneous characteristics, statistical characteristics, reproducibility

I. INTRODUCTION

There is a very widespread opinion that great French astronomer, mathematician, and physicist Pierre Simon de Laplace (1749–1827) declared: “Give me initial conditions and I will predict the future of the universe!”. Despite in reality he had never declared this (his statements were much lengthier and significantly more exact), we believe, however, that this statement is correct in the main, in a sense that the laws of nature are deterministic. This viewpoint is close to that of another great scientist Albert Einstein in his interpretation of the quantum-mechanical uncertainty principle: “God does not play dice with the universe”, he believed.[1] Note that the majority of modern theories using the notion of “chaos” proceed from the same assumption. It is possible to show that such a viewpoint leads us, in particular, to the notion of “deterministic turbulence (DeTu)”, whose existence in nature has been discovered recently in experimental fluid dynamics. It is very important to note that, in contrast to the well-known notion of “deterministic chaos”, which means the possibility of chaotic behavior of low-dimensional deterministic systems, the term “DeTu” refers to the possibility of deterministic behavior of very complex systems having practically an infinite number of degrees of freedom.

[a]Email: Bo@itam.nsc.ru.
[b]Corresponding author. Email: kachanov@itam.nsc.ru.

Why does chaos appear? Under the assumption of determinism of laws of nature postulated above, it was conjectured for many years that the appearance of chaotic properties of dynamical systems is associated with a great, in fact infinite, number of degrees of their freedom. For instance, movement of molecules in gases described by classical Gibbs statistics represents a perfect well known example. However, it has been found about 30 years ago, that the great number of degrees of freedom is not necessary at all for chaos origin.[2] It turned out that there are some broad classes of dynamical systems with a very low number of degrees of freedom, e.g., three ones, the strictly deterministic dynamics of which leads, however, to a chaotic behavior. This has been called "the deterministic (dynamic) chaos", which means a behavior of a low-dimensional dynamical system in a chaotic equilibrium, when this system walks "occasionally" among various states, although the laws of its evolution are deterministic, i.e., causal, and they are exactly described mathematically by rigorous equations. In phase space, i.e., a space defined by speeds and coordinates of fluid particles, the behavior of chaotic systems corresponds to a "strange (chaotic) attractor". This attractor represents a variety of phase trajectories, to which all other trajectories are attracted from a certain neighborhood of the attractor. The word "strange" emphasizes unusual properties of such attractors and, complexity of disjoint trajectories inside it, which corresponds to the chaotic behavior of the system. The appearance of the dynamic chaos is associated with the instability of dynamical systems, i.e., with the strong sensitivity of their behavior to initial and also boundary conditions. In phase space the instability is illustrated by a strong, usually exponential divergence of the phase trajectories occurring at finite time intervals even at small variation of the initial conditions.

Note that for ideal mathematical systems the only difference between the deterministic and chaotic dynamical systems is that the former are stable to initial and boundary disturbances, while the latter are unstable. However, in real systems everything occurs differently. Namely, there are no absolutely stable systems in nature! In other words, some indefinitely small disturbances are always present in all real systems. These disturbances will shift any real system from any stable state during a certain finite, maybe extremely large, time interval. This statement corresponds exactly to the well-known folk wisdom: "There is nothing permanent under the sun".

There is a philosophic deduction from the discussion, which has been formulated by one of the authors of the present paper as a hypothesis. We assume that all dynamical systems in nature develop according to deterministic laws and their behavior always has chaotic, i.e., stochastic, properties at large enough time scales, while at small enough time scales this behavior is basically deterministic, i.e., reproducible. Based on this assumption an obvious philosophical question arises. As far as the researchers have been astonished in the 70s by the fact that systems with a very small number of degrees of freedom, governed by deterministic laws, may have a chaotic behavior at certain, large enough but finite time scales, could it be possible that the behavior of real chaotic dynamical systems with a very large (nearly infinite) number of degrees of freedom be predictable, reproducible, deterministic in the main features at least at small but finite time scales?

An affirmative answer to this question was obtained experimentally several years ago, for turbulent flow of viscous incompressible fluids. The story of this important discovery is briefly described below (along with some new results related to properties of the DeTu found recently).

II. DISCOVERY OF DETERMINISTIC TURBULENCE

Various nonlinear mechanisms of boundary layer transition have been investigating for a long time during past several decades.[3–8] In particular, there was a long-term discussion about the scenarios of the transitional flow "randomization" which has to occur, as believed, at late stages of the boundary layer laminar-turbulent transition.[3] It was usually assumed by the term "randomization" that some broadband, uncontrolled disturbances have to grow rapidly and lead to appearance of stochastic turbulent motions inherent for fully turbulent flow. Meanwhile, some detailed experimental and numerical studies of late stages of transition, performed during past decade at more and more controlled disturbance conditions,[5–7] have not revealed any definite mechanisms of the final flow randomization. Moreover, the majority of the previously suggested mechanisms of the randomization[3] have been rejected by subsequent, more detailed, investigations. Therefore, a question appeared: "Is it possible that the instantaneous structure of transitional flow would remain deterministic, reproducible, and repeatable in the main (at repetition of the same initial conditions) at super-late, final stages of transition and even in the post-transitional fully turbulent boundary layer?" This question has been investigated in detail in the framework of several recent experiments.[8–11]

Those measurements were conducted in a flat plate boundary layer in presence of an adverse pressure gradient. The original laminar base flow was self-similar with constant Hartree parameter β_H equal to -0.115. The laminar-turbulent transition in this boundary layer occurred due to natural development of Tollmien–Schlichting (TS) waves. The uncontrolled background velocity disturbances were kept as low as it was possible, their root mean square (RMS) level was less than 0.04% of the free-stream velocity of about 9 m/s (in the frequency range above 1 Hz).

The controlled (reproducible) initial disturbances were introduced by means of a special generator. They represented a mixture of a quasi-2D TS-wave (corresponding to the most amplified one) and a broadband 3D disturbance consisted of a wide range of various TS-modes of the frequency-spanwise-wavenumber spectrum (Fig. 1). Downstream evolution of those controlled disturbances was natural. It started from the linear-instability amplification region, went through nonlinear stages, and ended with the fully turbulent state of the flow.

Despite a great complexity of the post-transitional turbulent boundary layer, it was shown to remain deterministic, basically, i.e., reproducible from one realization to another, for a certain distance, including those stages where the measured statistical characteristics corresponded already to the typical turbulent ones. It was possible to reproduce many times the instantaneous velocity field in the turbulent flow (Fig. 2).

The reproducibility, in turn, provided the possibility of performing detailed quantitative hot-wire measurements of the flow instantaneous structure under study. This important fact is illustrated in Fig. 3 by two instantaneous velocity disturbance fields measured in experiments two times: (1) in the morning and (2) in the evening of the same day.[11] The same, practically, instantaneous flow structure was reproduced during long experiment several millions of times and allowed performing ensemble averaging of the results of measurements extracting the reproducible, i.e., deterministic, component of the disturbance field.

One has to note that the investigation of the DeTu is very important because, in particular,

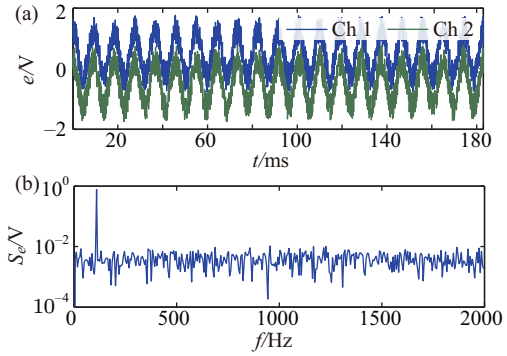

Fig. 1. (a) Two examples of signal time traces generated at channels 1 and 2 of the source and (b) the corresponding frequency spectrum averaged for all eight channels.[8]

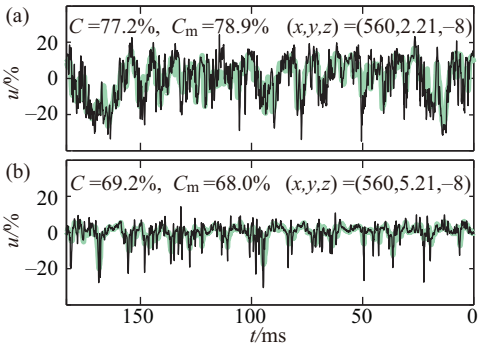

Fig. 2. Typical time-traces of total (thin black line) and ensemble-averaged (thick green line) velocity fluctuations measured at $x = 560$ mm at two distances from the wall.[8]

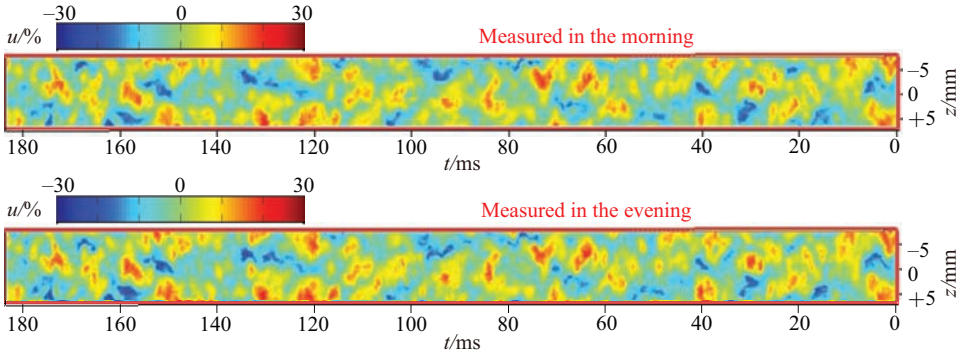

Fig. 3. Instantaneous fields of streamwise velocity disturbance measured in (z,t)-plane (plan view) at wall normal distance of 1 mm (close to the wall) measured (a) in the morning and (b) in the evening.[11]

it represents a powerful tool for both applied and fundamental studies. One of the first practical results obtained by means of this approach is illustrated in Fig. 4 obtained experimentally.[8] This figure displays some instantaneous velocity fields measured by a single hot-wire probe (point by point) in a post-transitional turbulent boundary layer in comparison with typical vortical structures observed in direct numerical simulation (DNS)[12] performed for a turbulent channel flow.

Moreover, a great power of the DeTu method has been shown recently in its first practical application[13,14] to investigation of one way to control wall-bounded shear flows by means of so-called large-eddy-break-up (LEBU) device. An instantaneous flow field $u(x,y,z,t)$ of the DeTu was documented in detail in those experiments in a boundary layer. Then some LEBU devices were installed (one after another) at a position, where the boundary layer was already practically turbulent, and the same instantaneous flow fields (but distorted by the presence of LEBU devices) were documented again. Detailed comparison of pairs of flow fields allowed the authors to investigate very clearly the physical mechanism of the LEBU device affect on the turbulent boundary layer. Examples of the instantaneous flow field distortion produced by one of the LEBU devices is illustrated in Fig. 5 for turbulent structures. There are four groups of (y,t)- and (y,z)-sections of two instantaneous streamwise-velocity fields measured without (Figs. 5(a1) and 5(b1)) and with (Figs. 5(a2) and 5(b2)) LEBU device at two streamwise locations $\Delta x = 20$ mm (Figs. 5(a)) and

50 mm (Figs. 5(b)) downstream the LEBU device trailing edge. Figure 5(a1) displays a ring-like vortex forming at $\Delta x = 20$ mm and two near-wall peaks of streamwise velocity fluctuations (skin-friction peaks) induced by it. The mechanism of formation of high-speed regions (called in Ref. 15 "positive spikes" and studied in Ref. 5) was investigated in detail and understood in Ref. 7. Mounting a LEBU device dissects the ring-like vortex and interrupts (or strongly perturbs) the process of its formation (Fig. 5(a2)).

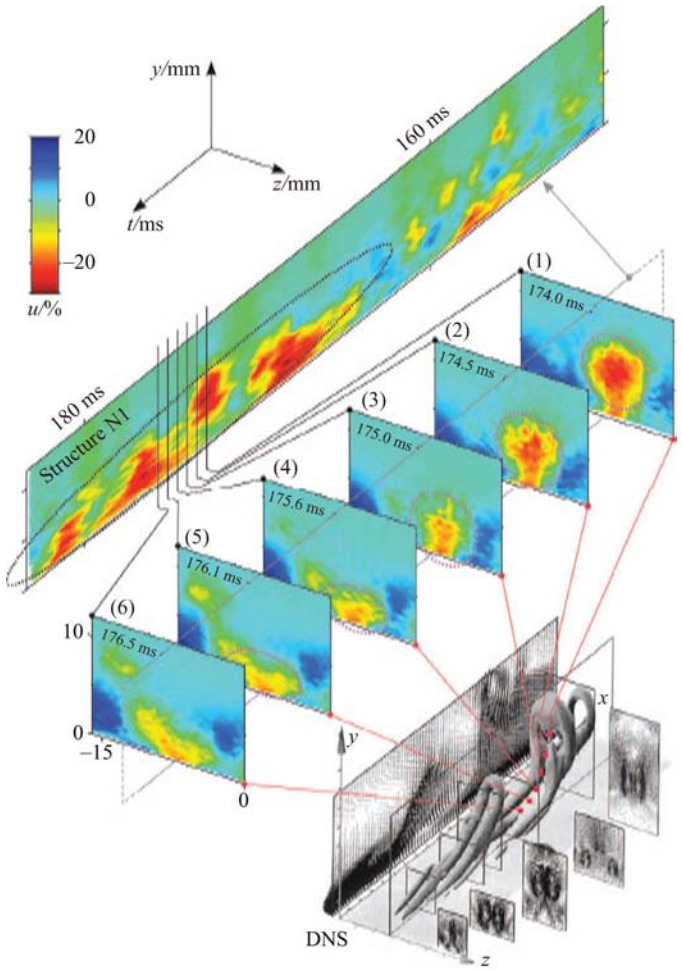

Fig. 4. Shape of one of vortical structures measured in post-transitional turbulent flow[8] (top and middle) in comparison with a turbulent structure calculated for channel flow[12] (bottom). Cross sections of instantaneous fields of streamwise-velocity fluctuations by (y,t)-plane (top) and by (y,z)-planes (middle).

Further downstream (at $\Delta x = 50$ mm) the same ring-like vortex remains rather strong in absence of LEBU device (Fig. 5(b1)), as well as the positive spikes (skin-friction peaks) induced by it in the near-wall region. Meanwhile, in the presence of LEBU device (Fig. 5(b2)) the ring-like vortex becomes much weaker and, hence, the skin-friction peaks (induced by this vortex) are reduced very significantly, as well (due to weakening the downward jets produced by the vortex ring[7]). This and many other similar results have helped to clarify the mechanism of acting the skin-friction reduction produced by LEBU devices.[13] Several other experiments like Ref. 13 are preparing at present based on the incredibly efficient method of DeTu.

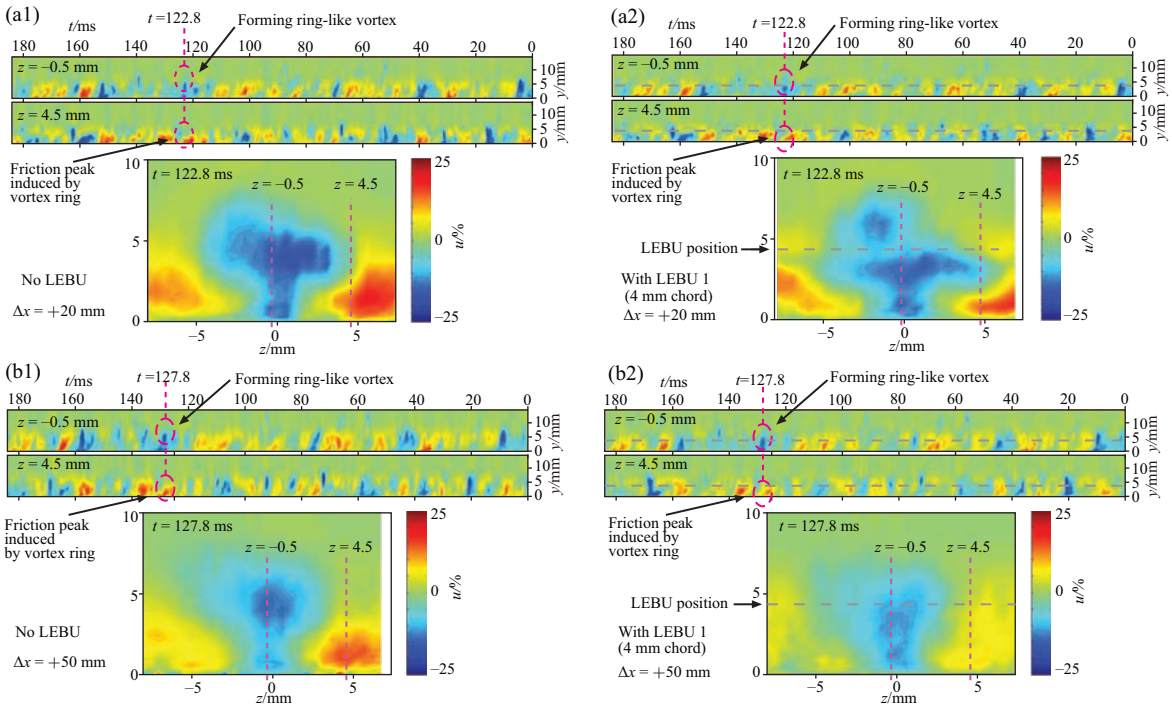

Fig. 5. Instantaneous fields of streamwise velocity disturbance measured in (y,t)-planes and their cross-section by (y,z)-planes obtained ((a1), (b1)) in absence of LEBU and ((a2), (b2)) in presence of LEBU 1 at a distance $\Delta x = 20$ mm and $\Delta x = 50$ mm downstream LEBU's trailing edge at $y = 4.2$ mm.

However, there were several questions related to the DeTu physical nature which remained unanswered. One of them was concerned to statistical characteristics of deterministic turbulent flows. Namely, if the DeTu corresponds exactly to the ordinary turbulent flow, these characteristics must be (1) independent of particular instantaneous realization of the DeTu and (2) identical to those of the ordinary (stochastic) turbulence. Another question was related to the DeTu instantaneous structure: (3) "To what extent the DeTu is the deterministic one?"

Results of recent experimental investigations presented below concentrated on the study of points (1) and (3). Thus, we have studied the Problem 1 of reproducibility of the DeTu statistical characteristics at variation of initial conditions from one realization to another and the Problem 2 of a degree of reproducibility of the DeTu instantaneous structure at its multiple reproductions from one realization to another at the same initial conditions.

III. PROCEDURES OF STUDY OF PROBLEMS 1 AND 2

Similar to the experiments discussed above, the new measurements were performed in a self-similar adverse-pressure-gradient (APG) boundary layer at fully controlled disturbance conditions at free-stream speed of about 9 m/s. The boundary layer developed over a flat plate surface and the APG was induced by a contoured wall bump mounted above the plate on the wind-tunnel test-section ceiling. The base-flow characteristics were similar to those studied in Refs. 8, 9, 11, 13, and 14 with the laminar boundary layer (in absence of the disturbance excitation) having Hartree

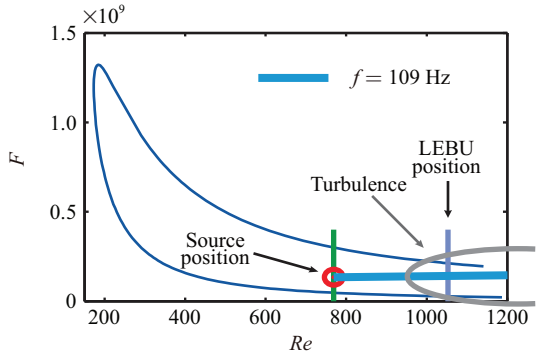

Fig. 6. Region of measurements with respect to the neutral stability curve (valid for primary laminar base flow).

parameter $\beta_H = -0.115$. The laminar-turbulent transition and the DeTu were produced due to natural development of TS-waves generated by a disturbance source, which excited in the flow a superposition of a harmonic 2D TS-wave and a broadband spectrum of 3D TS-waves (random in time and space) similar to those shown in Fig. 1.

Figure 6 demonstrates the region of measurements with respect to the neutral stability curve for the studied laminar base flow. The diagram is plotted in the coordinates of frequency parameter $F = 2\pi f\nu/U_{eo}^2$ versus Reynolds number $Re = U_{eo}\delta_{1o}/\nu$, where f is the 2D TS-wave frequency, ν is the air kinematic viscosity, U_{eo} is the mean-flow velocity at the boundary layer edge at the disturbance source location, and δ_{1o} is the boundary-layer displacement thickness at this location. The controlled initial disturbances were produced by a generator of TS-waves described in Ref. 8. The streamwise evolution of them started from their linear amplification, through nonlinear stages, and ending with the fully turbulent flow.

Within the framework of investigation of Problem 1 described above we have carried out, in fact, several experiments representing different realizations of the deterministic turbulent boundary layer. They have been named the experiments: A, B, C, AL1, BL1, CL1, AL2, BL2, and CL2. Letters A, B, and C designate three different particular realizations of initial signals excited by the disturbance source. The 2D TS-wave component was the same in all these three cases while the broadband 3D TS-wave components were different. Symbols L1 or L2 designate presence in the turbulent boundary layer of LEBU devices: either LEBU 1 or LEBU 2. These were thin metal plates located parallel to the surface at a distance of 4.2 mm from the wall and had chord lengths of 4 mm and 8 mm, respectively. The LEBU device trailing edge was always located at $x = 500$ mm. Every particular realization of the instantaneous flow structure was produced by a particular set of signals (either A or B or C) used for the boundary layer excitation. This instantaneous structure was reproduced hundreds thousand times (in every set of measurements) by means of a precise reproduction of initial disturbances and maintenance of the mean flow characteristics. Then we have analysed the constancy of statistical flow characteristics in different experiments, i.e., we have check independence of these characteristics from the particular instantaneous-flow structure.

During examination of Problem 2 we have carried out four experiments (named D, E, EL1, EL2) representing different realizations of the deterministic turbulent boundary layer. Characters D, E designate two different particular realizations of initial signals excited by the disturbance

source, while L1 and L2 designate presence in the flow of either LEBU 1 device or LEBU 2 device, respectively. We have analysed various properties of different flow realizations and concentrate on study of reproducibility of instantaneous flow structure at multiple reproduction of the same initial disturbance realization and, in particular, on dependence of irregular (non-reproducible) component of perturbations on the wall-normal, streamwise, and spanwise coordinates.

IV. PROBLEM 1: REPRODUCIBILITY OF STATISTICAL CHARACTERISTICS

A. Instantaneous disturbance fields

Two examples of measurement results for the "initial" instantaneous structure of the perturbed boundary layer flow, carried out at $x = 350$ mm (i.e., 50 mm downstream the disturbance source location) are shown in Fig. 7 for experiments A and B. Every plot is obtained by a single hot-wire probe after scanning (point by point) the flow field in the (y, z, t)-space. Thus, every plot represents just a cross-section of one of three arrays of experimental data related to the particular streamwise position $x = 350$ mm, which corresponds approximately to the initial nonlinear stage of the laminar-turbulent transition processes. The figure displays contours of constant values of the instantaneous streamwise velocity component.

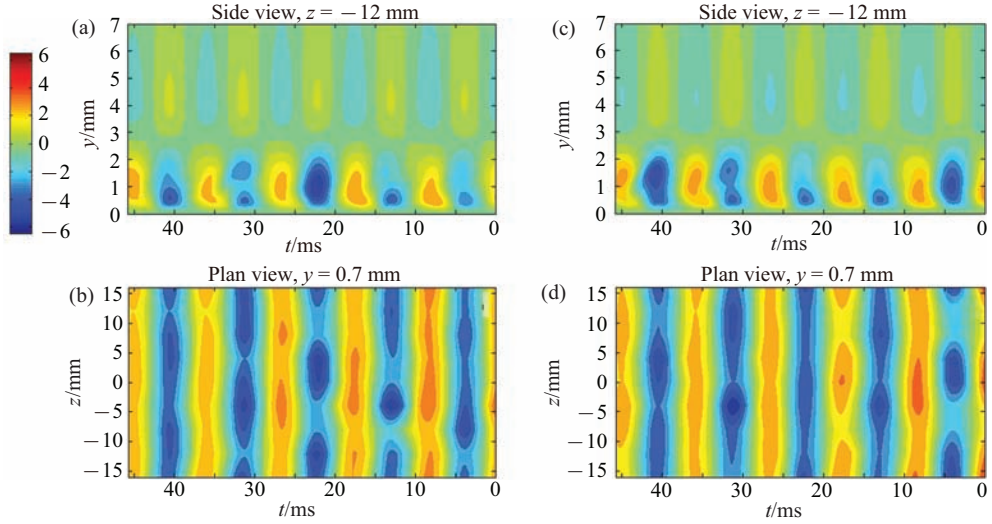

Fig. 7. Side and plan views of instantaneous streamwise-velocity field measured at "initial" streamwise position $x = 350$ mm in experiments A ((a), (b)) and B ((c), (d)).

It is seen that the difference of the particular realizations of the broadband components excited in experiments A and B (as well as in experiment C, which is not shown) results initially in significantly different 3D perturbations of the same 2D component of the excited TS-waves.

Further downstream the disturbance fields become very different, as a whole. For the same two experiments A and B, this point is illustrated in Fig. 8 ($x = 520$ mm) and Fig. 9 ($x = 550$ mm). These sections correspond practically to the fully developed deterministic turbulent boundary layer.

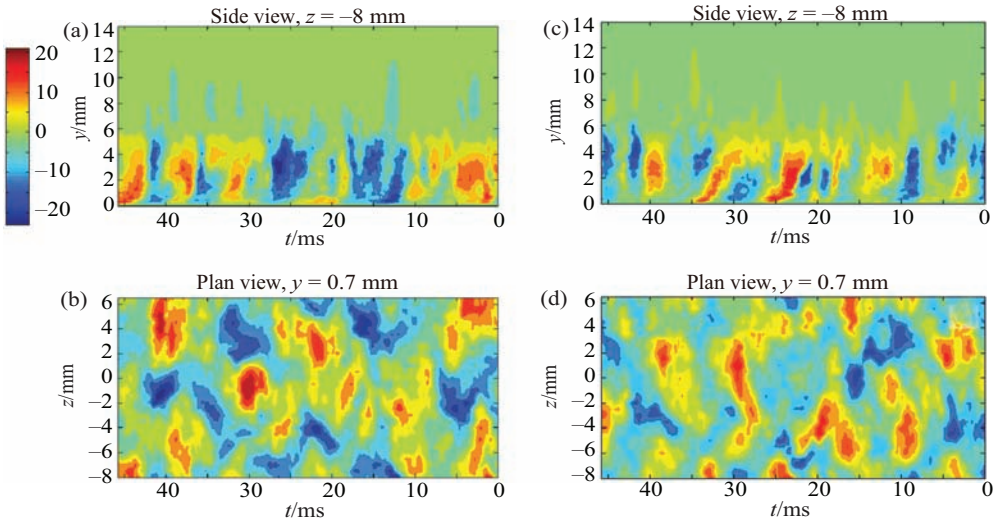

Fig. 8. Side and plan views of instantaneous streamwise-velocity field measured at streamwise position $x = 520$ mm in experiments A ((a), (b)) and B ((c), (d)).

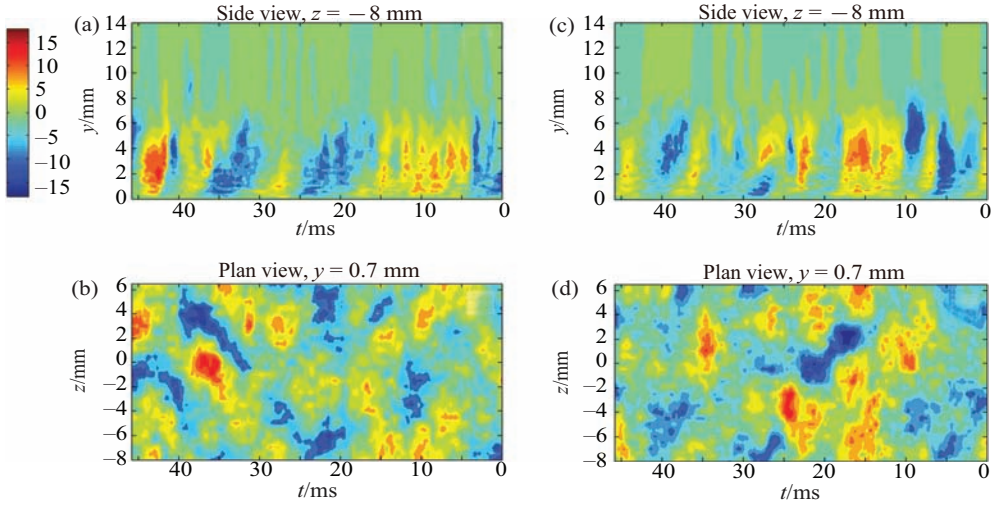

Fig. 9. Side and plan views of instantaneous streamwise-velocity field measured at streamwise position $x = 550$ mm in experiments A ((a), (b)) and B ((c), (d)).

Thus, it has been found that the instantaneous flow fields are very much different from each other in the discussed three experiments of excitation (A, B, and C) at these "late" streamwise locations, although a general character of the disturbance field remains the similar and looks like random one. Qualitatively similar results are obtained in triplets of experiments AL1, BL1, and CL1, as well as in AL2, BL2, and CL2 (not shown in figures).

B. Averaged characteristics

The profiles of the RMS-intensity of velocity fluctuations and the mean velocity profiles are the most important statistical characteristics of velocity fields in turbulent boundary layers. These

profiles have been measured for all studied experiments and compared with each other. Figure 10 shows the profiles obtained at $x = 350$ mm, 520 mm, and 550 mm in three experiments of excitation: A, B, and C. All profiles are averaged in time (during a rather short interval of 46 ms) and in the spanwise direction (in order to increase the accuracy of the measurements). It is seen that both the profiles of velocity fluctuations and the mean velocity profiles coincide practically with each other within a certain scattering of the experimental points (associated basically with a rather short time interval of averaging used). Similar results are observed for frequency spectra of streamwise-velocity disturbances presented in Figs. 11 and 12 for wall-normal distances $y = 1$ mm and $y = 4.5$ mm, respectively, for two groups of experiments: A, B, C (plots (a) and (c)) and AL1, BL1, CL1 (plots (b) and (d)), and for two streamwise locations: $x = 520$ mm (left pairs of plots) and 550 mm (right pairs of plots).

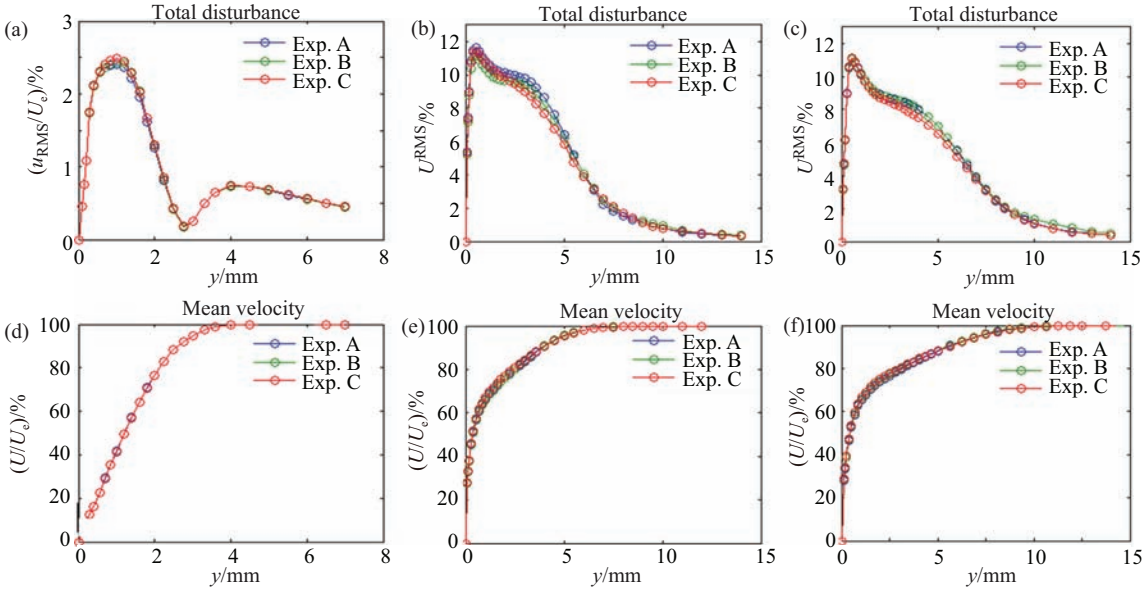

Fig. 10. Profiles of RMS-intensity of velocity fluctuations ((a)–(c)) and mean velocity ((d)–(f)) measured in experiments A, B, and C at initial nonlinear stage of laminar-turbulent transition ((a), (d), $x = 350$ mm), at stage of just formed DeTu ((b), (e), $x = 520$ mm), and at stage of developed DeTu ((c), (f), $x = 550$ mm).

The spectral shapes depends on wall-normal location and presence of LEBU device but are independent of the particular signal realization (A, B, or C), i.e., of the particular instantaneous structure of the deterministic turbulence.

C. Influence of LEBU devices

Note that in presence of LEBU devices the flow reproducibility remains almost the same as in absence of them. Moreover, close to the LEBU device (at $x = 520$ mm) even the instantaneous flow structure remains almost the same as that measured without LEBU (excluding the wall-normal distance of the LEBU location at $y = 4.2$ mm) if the same signals are used for the boundary layer excitation. This fact is illustrated by comparison of the instantaneous velocity-field cross-

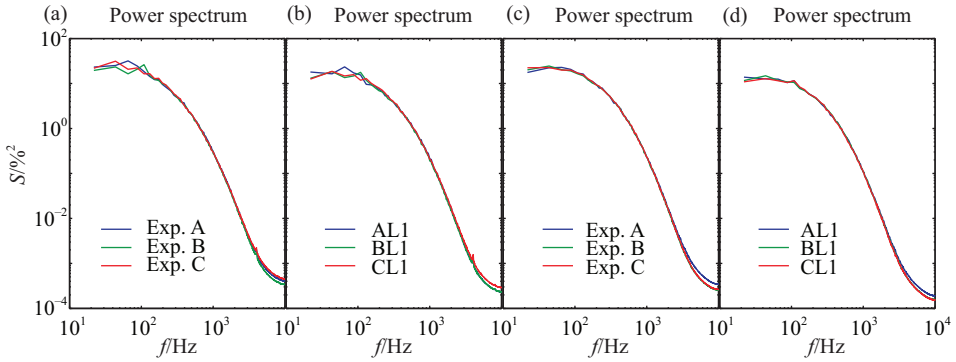

Fig. 11. Frequency spectra of velocity fluctuations measured in experiments A, B, and C ((a) and (c)) and AL1, BL1, and CL1 ((b) and (d)) at stages of just formed ((a), (b), $x = 520$ mm) and developed ((c), (d), $x = 550$ mm) DeTu. Wall-distance $y = 1.0$ mm.

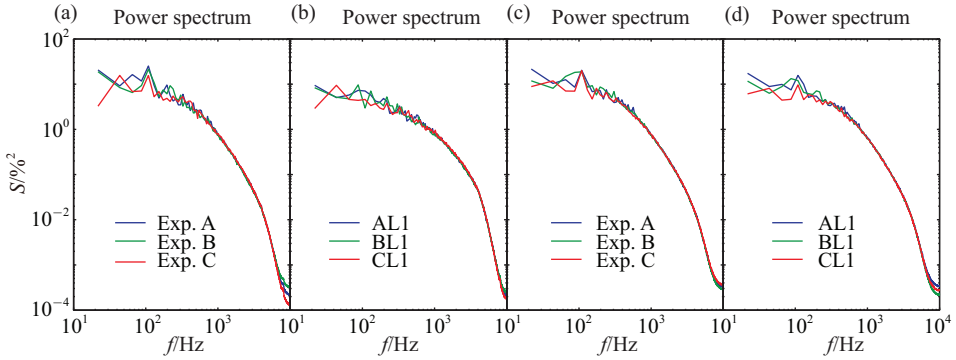

Fig. 12. Frequency spectra of velocity fluctuations measured in experiments A, B, and C ((a) and (c)) and AL1, BL1, and CL1 ((b) and (d)) at stages of just formed ($x = 520$ mm, (a) and (b)) and developed ($x = 550$ mm, (c) and (d)) DeTu. Wall-distance $y = 4.5$ mm.

sections obtained in experiment AL1 (Fig. 13), which look very similar to those measured in the corresponding experiment A (Figs. 8(a) and 8(b)) in absence of LEBU. Similar agreement is observed for the instantaneous fields measured in pairs of experiments B, BL1 and C, CL1 (not show in plot). And again, profiles of the velocity fluctuations and the mean-velocity profiles display their independence practically from the particular instantaneous structure produced by every particular set of signals used for the disturbance source excitation (Figs. 14(a) and 14(b), 11(b), and 12(b)).

Similar result is observed further downstream, at $x = 550$ mm in presence of both LEBU 1 (Figs. 14(c) and 14(d), 11(d), and 12(d)) and LEBU 2 devices (not shown in the plot).

Thus, it is found that variation of initial disturbance conditions changes significantly the instantaneous structure of the post-transitional deterministic turbulent flow. However, the most important statistical characteristics of all studied flow realizations turned out to remain practically the same and are typical to those of the regular (stochastic) turbulent boundary layer.

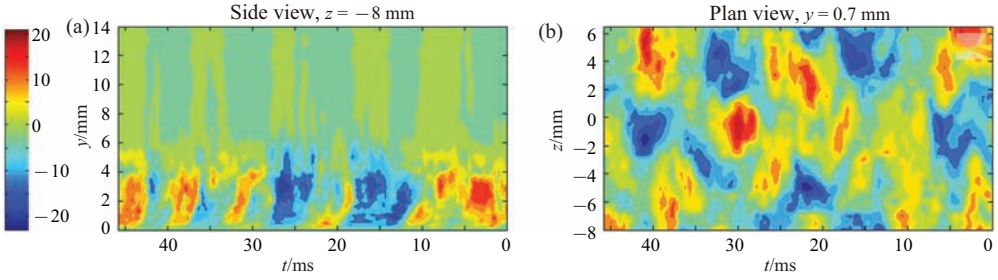

Fig. 13. Side and plan views of instantaneous streamwise-velocity field measured at streamwise position $x = 520$ mm in experiment AL1.

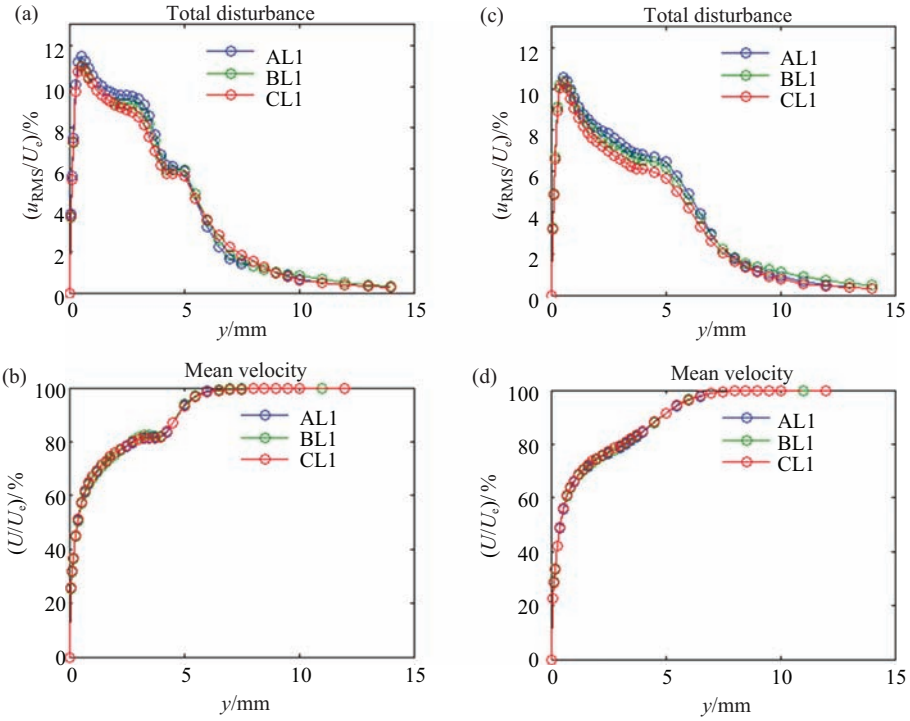

Fig. 14. Profiles of RMS-intensity of velocity fluctuations ((a) and (c)) and mean velocity ((b) and (d)) measured in experiments AL1, BL1, and CL1 at stage of deterministic turbulent boundary layer just downstream LEBU 1 device ((a), (b), $x = 520$ mm) and farther downstream ((c), (d), $x = 550$ mm).

V. PROBLEM 2: REPRODUCIBILITY OF INSTANTANEOUS STRUCTURE

A. General evolution of disturbance fields

Figures 15–18 illustrate streamwise evolution of a set of fields (in the (y,z)-plane) of RMS-intensity of full (total, A_t), deterministic (i.e., reproducible obtained after ensemble averaging, A_d), and unreproducible (random, $A_r = A_t - A_d$) components of boundary layer streamwise-velocity disturbances measured in experiment E at four successive stages of evolution of the transition process. The fields presented in Figs. 15 and 16 correspond to two stages of boundary layer transition, while Figs. 17 and 18 are measured in a post-transitional turbulent boundary layer. The corresponding mean-velocity fields are also presented in these figures (plot (d)). The results are

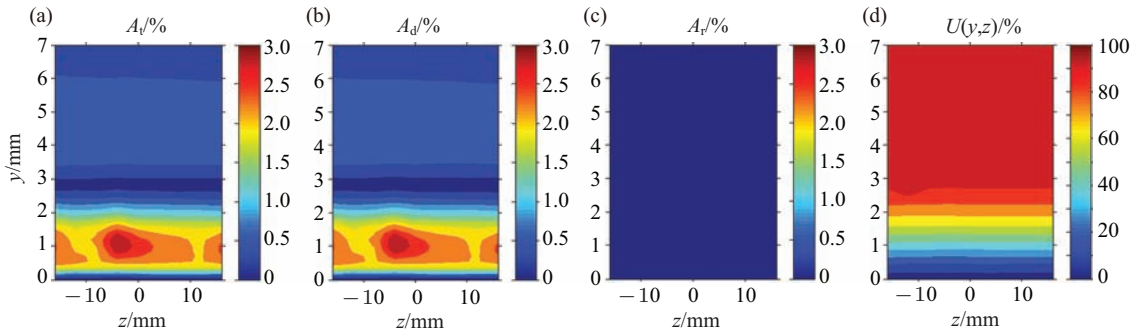

Fig. 15. Fields of RMS-intensity of (a) total, (b) deterministic, and (c) random components of boundary layer disturbances measured at "initial" streamwise position $x = 350$ mm in experiment E. Contours of mean flow velocity are shown in plot (d).

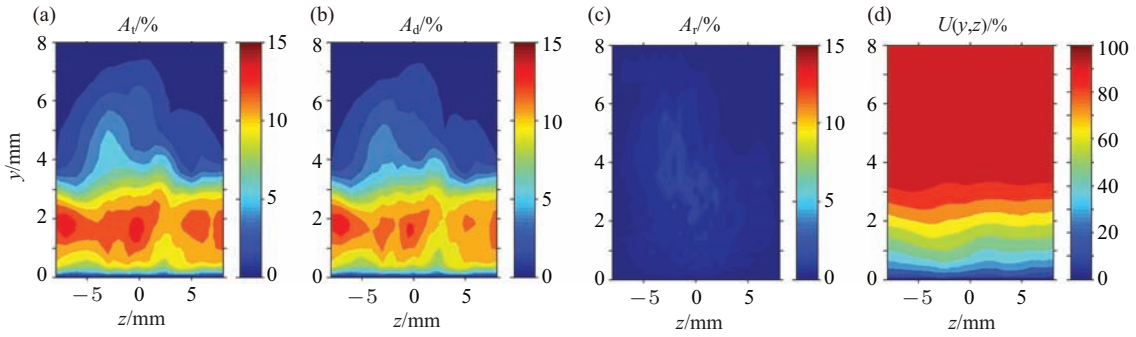

Fig. 16. Fields of RMS-intensity of (a) total, (b) deterministic, and (c) random components of boundary layer disturbances measured at late stage of transition ($x = 450$ mm) in experiment E. Contours of mean flow velocity are shown in plot (d).

obtained based on ensemble averaging of 20 velocity time traces having length of 0.183 s each consisting of 20 periods of the fundamental TS wave. This length corresponds to a period of repetition of controlled broadband component of the signal used for disturbance excitation.

It is seen that in the transitional boundary layer (including very late stage shown in Fig. 16), the flow remains quite reproducible; the total (plot (a)) and deterministic (plot (b)) disturbance fields coincide practically with each other, while the unreproducible perturbations (plot (c)) remain very weak at these stages at all values of the spanwise and wall-normal coordinates. Farther downstream the intensity of random perturbations increases (Figs. 17(c) and 18(c)), especially in the wall region, although the deterministic component remains predominant almost in the whole flow.

Qualitatively similar results are observed in other studied experiments. This fact is illustrated in Figs. 19–21 displaying results of measurements performed at $x = 520$ mm in experiment EL1 (20 mm downstream from LEBU 1 device) and at $x = 550$ mm in experiments EL1 and EL2 (50 mm downstream from LEBU 1 and LEBU 2 devices). Note that at $x = 520$ mm (Fig. 19) the presence of LEBU device changes very little the fields of all three components of the velocity disturbances. Main distinctions are observed only immediately in the wake of the LEBU device (around $y = 4.2$ mm); the reproducibility of the disturbance field is somewhat weaker there. Similar tendencies are seen farther downstream (Figs. 20 and 21), while the influence of the LEBU

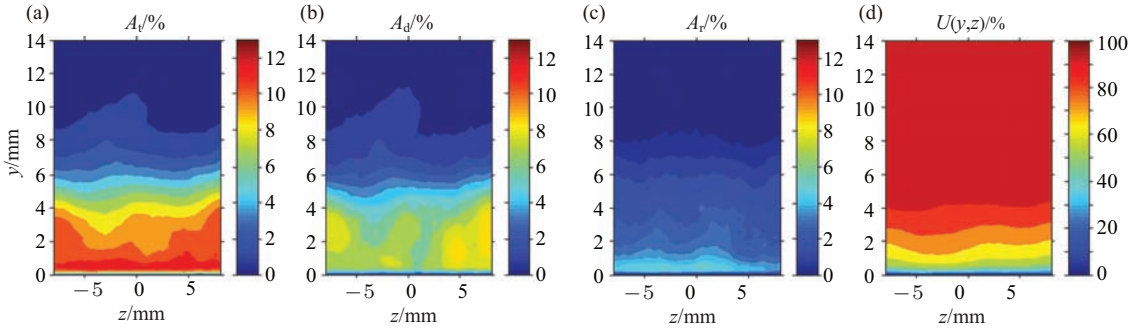

Fig. 17. Fields of RMS-intensity of (a) total, (b) deterministic, and (c) random components of boundary layer disturbances measured at stage of just formed deterministic turbulent boundary layer ($x = 520$ mm) in experiment E. Contours of mean flow velocity are shown in plot (d).

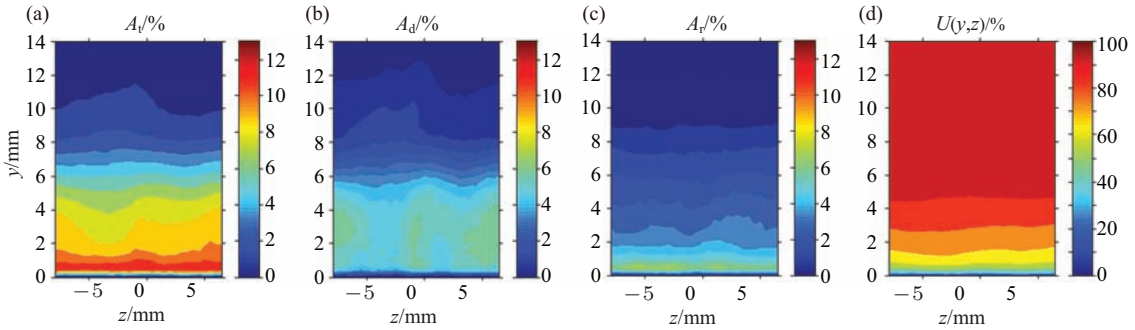

Fig. 18. Fields of RMS-intensity of (a) total, (b) deterministic, and (c) random components of boundary layer disturbances measured at stage of developed deterministic turbulent boundary layer ($x = 550$ mm) in experiment E. Contours of mean flow velocity are shown in plot (d).

devices spreads in the wall-normal direction, especially towards the wall, leading to reduction of the disturbance intensity.

B. Properties of wall-normal disturbance profiles

Some quantitative information about the wall-normal distributions of RMS-intensities of the total, deterministic, and random components of the streamwise-velocity perturbations is presented in Figs. 22–27 for experiment E at one of fixed spanwise locations for several streamwise positions (between $x = 350$–590 mm).

Mean velocity profiles shown in Fig. 22 display that the shape of the profiles evolves gradually from laminar to turbulent one. Starting from streamwise coordinate $x \approx 500$ mm, the shape is stabilized, and does not evolve any more and becomes typical for the developed turbulent flow.

The wall-normal profiles of RMS-intensity of total velocity fluctuations (Fig. 23) evolve from those characteristic for a quasi-2D TS-wave to those typical for the developed turbulent boundary layer. The shape is also stabilized after $x \approx 500$ mm; further evolution is associated, basically, with a slow reduction of the disturbance intensity. A characteristic strong maximum of fluctuation amplitudes is observed very near the wall and has value of about 12% which is also very typical for the developed turbulent boundary layers.

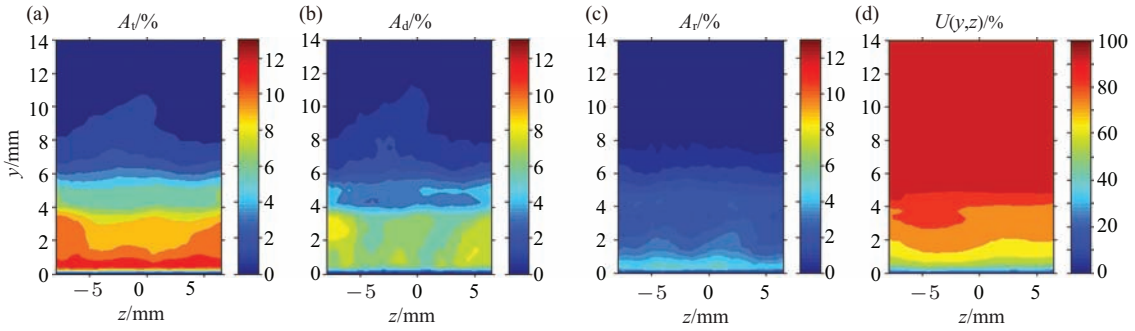

Fig. 19. Fields of RMS-intensity of (a) total, (b) deterministic, and (c) random components of boundary layer disturbances measured at stage of just formed deterministic turbulent boundary layer ($x = 520$ mm) in experiment EL1. Contours of mean flow velocity are shown in plot (d).

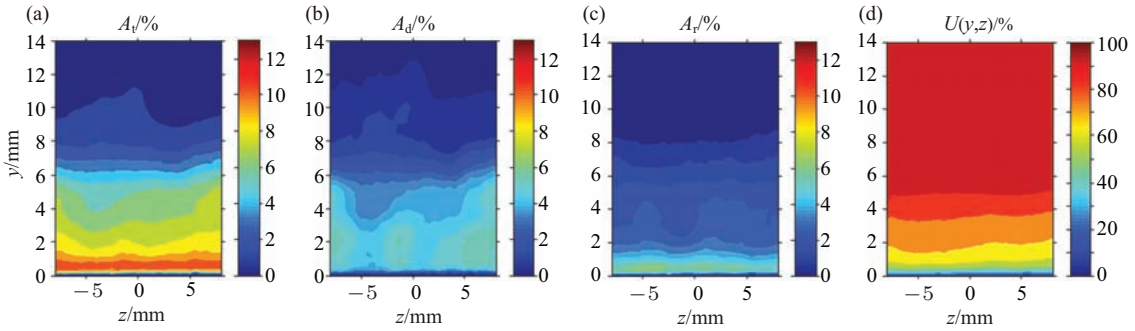

Fig. 20. Fields of RMS-intensity of (a) total, (b) deterministic, and (c) random components of boundary layer disturbances measured at stage of developed deterministic turbulent boundary layer ($x = 550$ mm) in experiment EL1. Contours of mean flow velocity are shown in plot (d).

The evolution of the shape of wall-normal amplitude profiles of the deterministic (reproducible) component of the streamwise velocity fluctuations is illustrated in Fig. 24 for the same experiment E. This shape is rather similar to that of the profiles of total velocity fluctuations (shown in Fig. 23). The most significant difference is attributed to a smaller magnitude of fluctuations, especially in the near-wall region. The rate of the downstream reduction of amplitude of the deterministic component of fluctuations is also greater than for the total disturbance.

The corresponding set of wall-normal profiles of the random (unreproducible) component of

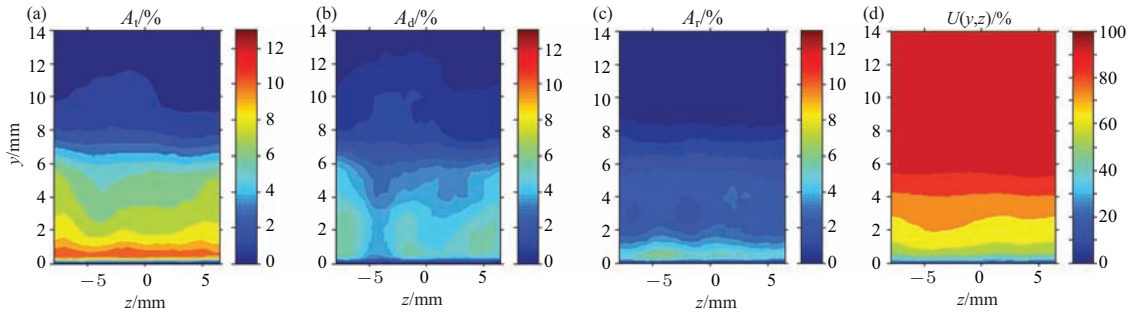

Fig. 21. Fields of RMS-intensity of (a) total, (b) deterministic, and (c) random components of boundary layer disturbances measured at stage of developed deterministic turbulent boundary layer ($x = 550$ mm) in experiment EL2. Contours of mean flow velocity are shown in plot (d).

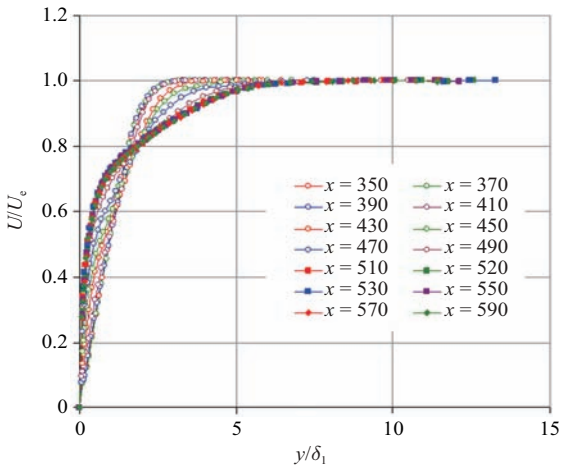

Fig. 22. Streamwise evolution of profiles of mean flow velocity measured in experiment E at $z = -2$ mm.

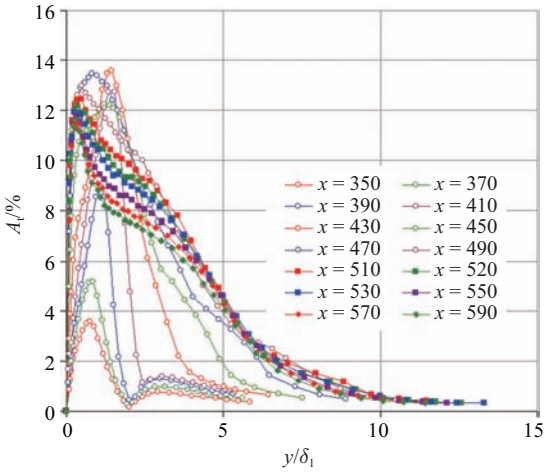

Fig. 23. Streamwise evolution of profiles of total RMS-intensity of flow-velocity fluctuations measured in experiment E at $z = -2$ mm.

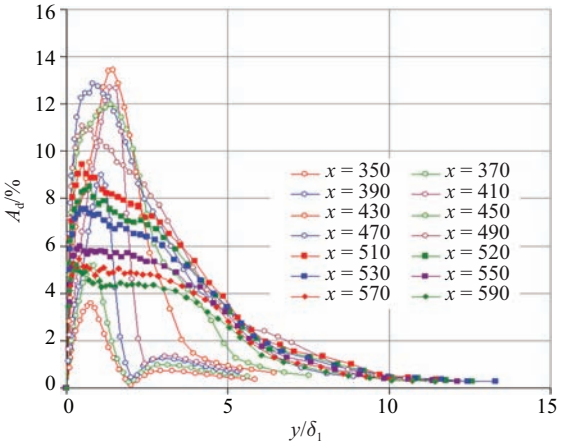

Fig. 24. Streamwise evolution of profiles of RMS-intensity of deterministic component of flow-velocity fluctuations measured in experiment E at $z = -2$ mm.

velocity fluctuations is presented in Fig. 25(a) (again for experiment E). Almost in the entire region of boundary layer transition, including part of late stages (until $x \approx 470$ mm), the largest amplitudes of the random component of velocity perturbations are observed rather far from the wall, between $y \approx 2$–3 mm. However, after $x \approx 490$ mm, when the post-transitional turbulent flow appears, the maximum of unreproducible disturbances jumps to the near-wall region and remains there farther downstream. The amplitudes of these uncontrolled perturbations increase downstream.

The relationship between amplitudes of all three kinds of velocity perturbations is visually illustrated in Fig. 26 for three successive stages of evolution of post-transitional turbulent boundary layer (at $x = 510$ mm, $x = 520$ mm, and $x = 530$ mm). It is seen that the deterministic (reproducible) disturbances are predominant at these stages of flow development, although random (unreproducible) perturbations grow downstream, while the deterministic ones decay.

The shapes of wall-normal profiles of total and deterministic perturbations are very similar to

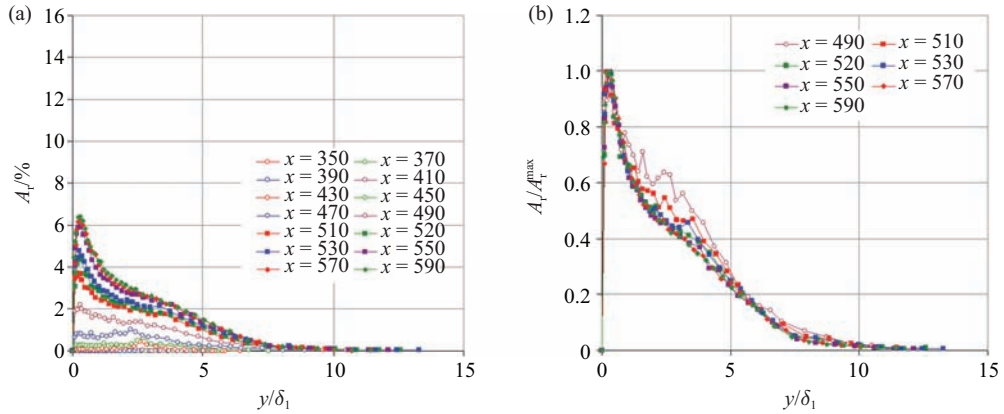

Fig. 25. (a) Streamwise evolution of profiles of RMS-intensity of random (unreproducible) component of flow-velocity fluctuations and (b) their self-similarity in turbulent streamwise region. Experiment E, $z = -2$ mm.

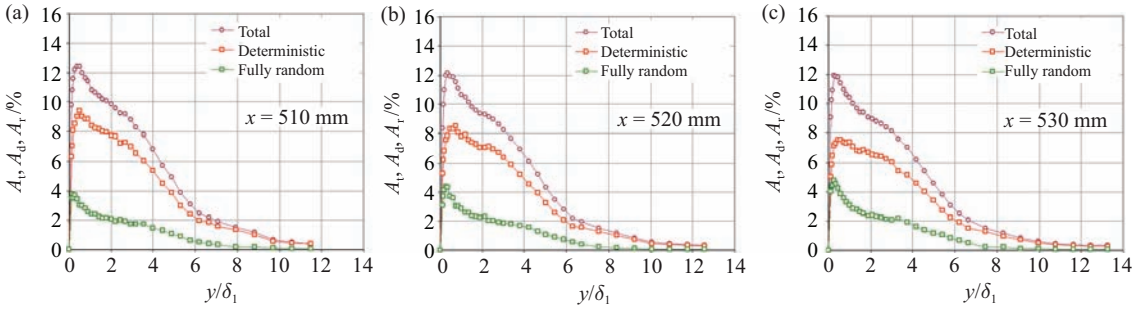

Fig. 26. Comparison of wall-normal profiles of RMS-intensity of three kinds of velocity perturbations: (a) total, (b) deterministic, and (c) random, measured at (a) 510 mm, (b) 520 mm, and (c) 530 mm. Experiment E, $z = -2$ mm.

each other, although the sharpness of the near-wall amplitude peak of the deterministic perturbations gets weaker by $x = 530$ mm compared to that of total disturbances. Meanwhile, the sharpness of the near-wall maximum of profiles of the random (unreproducible) disturbances remains rather strong after $x \approx 500$ mm and the shape of the profiles becomes self-similar (Fig. 25(b)), although somewhat different from that of the total velocity disturbance profiles.

C. Disturbance amplification curves

The amplification curves of RMS amplitudes of all three kinds of velocity perturbations are presented in Fig. 27 for experiments E and D. It is seen that the total disturbance amplitude saturates at $x \approx 430$ mm in experiment E and at $x \approx 470$ mm in experiment D. Farther downstream it decays slowly in a monotonous way. The amplitude of the deterministic component of perturbations displays the same behavior initially but deviates slowly from the total amplitude in the end. The amplitude of the random (unreproducible) disturbance component increases in an exponential way for a long distance and then saturates when it approaches the amplitude of the deterministic component. Note that both the shape of wall-normal profiles and the exponential character of am-

plification of the unreproducible component of perturbations are in a good agreement with those found in numerical simulation in Ref. 16.

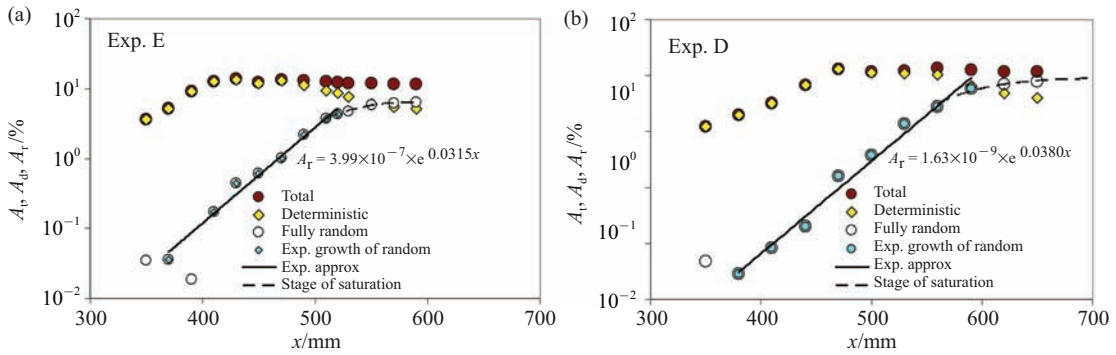

Fig. 27. Amplification curves of RMS-intensity of three kinds of velocity perturbations: total, deterministic, and random ones measured in experiments E ((a) $z = -2$ mm) and D ((b) $z = -8$ mm). $y = y_{max}$ (individual for every mode).

VI. CONCLUSIONS

Based on the experimental results discussed above the following most important conclusions can be drawn:

(1) The deterministic turbulence is a reality, which existence in nature is proved experimentally.

(2) The deterministic turbulence method is a very powerful tool for experimental turbulence research without a rival.

(3) It is found that variation of initial disturbance conditions changes significantly the instantaneous structure of the deterministic turbulent flow (as expected), while the most important statistical characteristics of all studied flow realizations turned out to remain the same and are typical to those of the regular (stochastic) boundary layer turbulence.

(4) The unreproducible, fully irregular uncontrolled perturbations grow unavoidably in the post-transitional flow and transform gradually the deterministic turbulent flow into the regular, stochastic one. The amplitudes of these irregular disturbances grow downstream exponentially (in a qualitative agreement with temporal DNS by Nikitin[16]).

(5) The wall-normal profiles of unreproducible disturbances are self-similar and have an extremely sharp peak very near the wall.

This work was supported by the budget of the Russian Academy of Sciences.

1. M. Born, I. Born. The Born–Einstein Letters. Walker Publishing Company, New York (1971).
2. J. P. Crutchfield, J. D. Farmer, N. H. Packard, et al. *Chaos. Sci. Am.* **254**, 46–57 (1986).
3. Y. S. Kachanov. Physical mechanisms of laminar-boundary-layer transition. *Ann. Rev. Fluid Mech.* **26**, 411–482 (1994).

4. V.I. Borodulin, Y.S. Kachanov, D.B. Koptsev. Experimental study of resonant interactions of instability waves in self-similar boundary layer with an adverse pressure gradient: I. Tuned resonances. *Journal of Turbulence* **3**, N62 (2002).
5. V. I. Borodulin, V. R. Gaponenko, Y. S. Kachanov, et al. Late-stage transitional boundary-layer structures. Direct numerical simulation and experiment. *Theoret. Comput. Fluid Dynamics* **15**, 317–337 (2002).
6. V. I. Borodulin, Y. S. Kachanov, A. P. Roschektayev. Turbulence production in an APG-boundary-layer transition induced by randomized perturbations. *Journal of Turbulence* **7**, 1–30 (2006).
7. H. Guo, V. I. Borodulin, Y. S. Kachanov, et al. Nature of sweep and ejection events in transitional and turbulent boundary layers. *Journal of Turbulence* **11**, N34 (2010).
8. V. I. Borodulin, Y. S. Kachanov, A. P. Roschektayev. Experimental detection of deterministic turbulence. *Journal of Turbulence* **12**, 1–34 (2011).
9. V. I. Borodulin, Y. S. Kachanov, A. P. Roschektayev. The deterministic wall turbulence is possible. Proc. 11th European Turbulence Conference. Porto, Portugal, June 25–28 (2007).
10. Y. S. Kachanov. Hypothesis on deterministic turbulence. *Eur. J. Mech., B/Fluids* **32**, 1–4 (2013).
11. V.I. Borodulin, Y.S. Kachanov. Experimental evidence of deterministic turbulence. *Eur. J. Mech., B/Fluids* **32**, 5–11 (2013).
12. J. Zhou, R.J. Adrian, S. Balachandar, T.M. Kendal. Mechanisms for generating coherent packets of hairpin vortices in channel flow. *J. Fluid Mech.* **387**, 353–396 (1999).
13. V. I. Borodulin, Y. S. Kachanov, A. P. Roschektayev. Investigation of LEBU-device effect on turbulent boundary layer structure by means of "deterministic turbulence method". Proceedings of 14th International Conference on Methods of Aerophysical Research. June 30 – July 6, Novosibirsk (2008).
14. V.I. Borodulin, Y.S. Kachanov, A.P. Roschektayev. Application of the deterministic turbulence method to study of LEBU-device mechanism. *Springer Proceedings in Physics* **132**, 313–316 (2009).
15. V.I. Borodulin, V.R. Gaponenko, and Y.S. Kachanov. Generation and development of coherent structures in boundary layer at pulse excitation. Proceedings of 10th International Conference on Methods of Aerophysical Research. Novosibirsk (2000).
16. N.V. Nikitin. On the rate of spatial predictability in near-wall turbulence. *J. Fluid Mech.* **614**, 495–507 (2008).